

Effect of Tensile Strain Rate on the Mechanical Properties of Constrained-Uniaxially and Simultaneous-Biaxially Drawn Poly(ethylene Terephthalate) Sheets

MITSURU YOKOUCHI, JUNICHIRO MORI, and YASUJI KOBAYASHI,
*Department of Industrial Chemistry, Faculty of Technology, Tokyo
Metropolitan University, Fukazawa, Setagaya-ku Tokyo 158, Japan*

Synopsis

The dependency of the mechanical properties (Young's modulus, yield strength, breaking strain, and breaking energy) of preoriented poly(ethylene terephthalate) (PET) sheets on the tensile deformation speeds was examined and discussed in relation to changes of density and birefringence. The procedures for preorientation were constrained-uniaxially (CU) and simultaneous-biaxially (SB) drawings at 65°C. The performance characteristics of the present tensile testing at room temperature were obtained over a wide range of extension rates (1.7×10^{-4} – 13.1 m/s = 0.29 – 2.3×10^4 %/s) without changing the mode of deformation and the shape of the test pieces. The CU drawn PET is strain-rate-independent and mechanically superior in structure in the preextended direction with draw ratio $\lambda > 2.5$. In the SB drawn PET such a structure comes into existence at $\lambda > 3$, which has, furthermore, no dependency on draw direction (mechanically isotropic). The draw ratio of the latter case corresponded to the birefringence ($-\Delta n/d$) of about 5×10^{-2} . These results imply a possibility of producing the strain rate (from low to impact speeds) independent, anisotropy-free, and mechanically superior molded products of PET if adequate extrusion or blow molding methods which induce multiaxial orientation with $-\Delta n/d > 5 \times 10^{-2}$ are developed.

INTRODUCTION

When applying external forces in a wide range of speeds, molded plastic products should be strain-rate-independent and maintain mechanically superior properties. In choosing plastic materials, it is important to perform uniform tensile breaking tests from low to impact extension rates. Accordingly, we have manufactured a new flywheel-type tensile impact tester for polymer sheet and film.¹ This apparatus and the conventional tensile tester enabled us to test over five decades of deformation speeds without changing the mode of deformation or the shape of the test pieces. Its application to several polymers has already been reported.²⁻⁴ For example, polycarbonate (PC) as an undrawn material is strain-rate-independent and has excellent properties (Young's modulus 5 GPa, tensile strength 100 MPa, and breaking energy $7 \text{ MJ}\cdot\text{m}^{-2}$ approximately constant between low and impact speeds).⁴ On the other hand, undrawn amorphous poly(ethylene terephthalate) (PET) shows the same properties as PC in the lower speed region, while its impact properties become increasingly worse; the failure mode turns from ductile to brittle (breaking energy $0.2 \text{ MJ}\cdot\text{m}^{-2}$). In the previous paper,² however, uniaxially drawn PET at the draw ratios (λ) more than 2.3 showed improvement in its impact strength and compared favorably with PC. The present paper describes the results of more detailed tensile testing at various

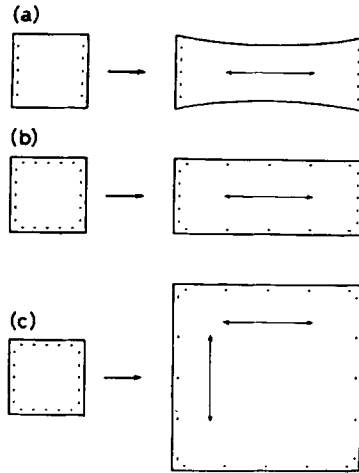


Fig. 1. Three pre-extension methods: (a) sideway free uniaxial; (b) constrained uniaxial; and (c) simultaneous biaxial.

draw ratios and a wide range of deformation speeds for constrained-uniaxially and simultaneous-biaxially drawn PET sheets. If specific drawing methods are found to induce a mechanically superior structure which behaves as PC in the range from low to impact strain rates, increased demand for PET will be realized.

EXPERIMENTAL

Specimens

Undrawn and quench-rolled PET, supplied by TeijinCo., Ltd., was used as a starting material throughout this study (260- μm thickness and density 1.344 $\text{g}\cdot\text{cm}^{-3}$). This sheet was isotropic, with no orientation observed by an optical

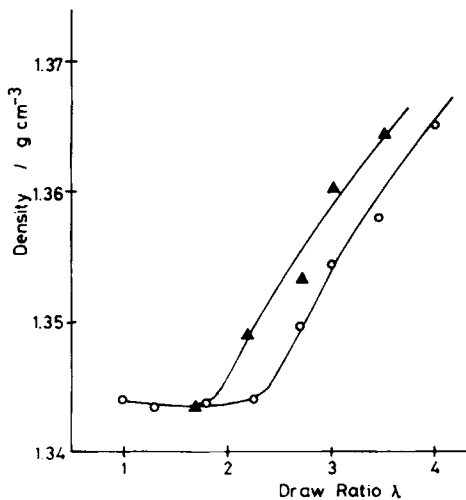


Fig. 2. Variation of density with draw ratio for PET sheet: (○) constrained uniaxially; (▲) simultaneous biaxially.

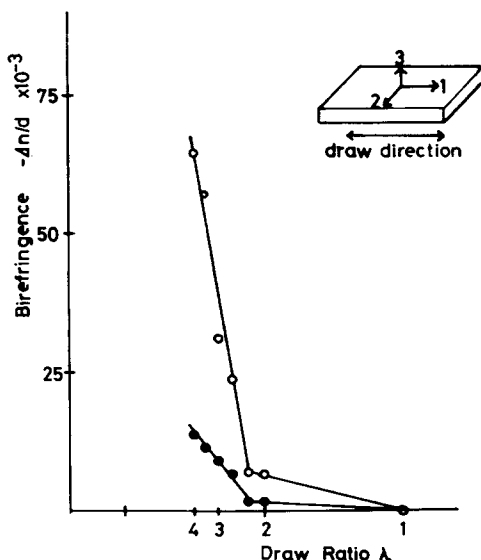


Fig. 3. Change of birefringence with draw ratio for the constrained-uniaxially drawn PET sheet: (○) $-\Delta n/d(\parallel) = (n_3 - n_1)/d$; (●) $-\Delta n/d(\perp) = (n_3 - n_2)$.

microscope. In order to obtain samples of different orientation, the sheets were placed in an air oven in the biaxially stretching machine at 65°C for 6 min and drawn constrained-uniaxially (CU) and simultaneous-biaxially (SB) to various lengths, followed by cooling to room temperature (Fig. 1). The draw ratios (λ) were up to 4 in the former case, and up to 3.5 in the latter case at intervals of 0.5 (further elongation invariably resulted in sample rupture). Specimens for tensile and impact tensile testing (the substantial dimensions 5×58 mm) were prepared from the above elongated sheets. The cut-out angles (θ) to the preextended direction (the direction 1 described later) were 0° (\parallel) and 90° (\perp) for the CU drawn sheets, and 0°, 22.5°, and 45° for the SB drawn sheets, respectively.

Density

Density of the samples were measured at 23°C in a density gradient column composed of *n*-heptane and carbon tetrachloride. After soaking in the column, the position of the specimen was read at intervals of 1, 2, 4, 8, and 16 min and then plotted against the reciprocal of the root of the measurement time. The observed density was estimated by extrapolation of the curve to infinite time.

Birefringence

Refractive index measurements of the samples (n) were carried out with α -bromonaphthalene, using an Abbe refractometer at room temperature. The values of birefringence were defined as follows (see Figs. 3, 11): (1) for the CU drawing, $-\Delta n/d(\parallel) = (n_3 - n_1)/d$ and $-\Delta n/d(\perp) = (n_3 - n_2)/d$; and (2) for the SB drawing, $-\Delta n/d = (n_3 - n_1)/d = (n_3 - n_2)/d$, where d is an observed density and the subscript 1 corresponds to the drawing direction, the subscript 2 to the sideway direction, and the subscript 3 to the direction perpendicular to 1 and

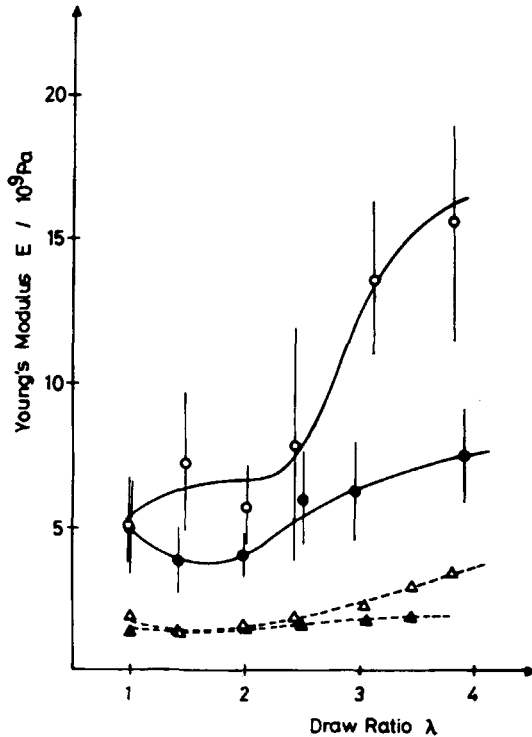


Fig. 4. Dependence of Young's modulus on draw ratio λ and extension rate $\dot{\epsilon}$ for the constrained-uniaxially drawn PET sheet: (O) (||), (●) (\perp) at $\dot{\epsilon} = 227 \text{ s}^{-1}$; (Δ) (||), (\blacktriangle) (\perp) at $\dot{\epsilon} = 2.9 \times 10^{-3} \text{ s}^{-1}$.

2, respectively. Accordingly, the stretching directions of 1 and 2 are equivalent ($n_1 = n_2$) in the case of SB drawing.

Tensile Breaking Tests

For the lower speed tensile testing, a conventional tensile tester was utilized, which covered the rate of deformation from 1.7×10^{-4} to 2.8×10^{-2} m/s. For the higher speeds, a flywheel-type impact tensile tester was used.¹ The tensile speeds could be easily controlled by changing the revolutions of the flywheel, and in the present study were adopted for the range of 1.3–13.1 m/sec. These enabled us to test over five decades of strain rate (1.7×10^{-4} –13.1 m/s = 0.29 – 2.3×10^4 %/s). The experiments were conducted at 23°C and below a relative humidity of 50%. The numbers of specimens tested per each strain rate were nine for the higher speeds and five for the lower speeds (due to the small scattering of data points in the latter case). The arithmetic mean and estimated standard deviation were calculated from the set observations. The stress-strain curves gave the following four mechanical quantities: (1) modulus of elasticity E ; (2) tensile stress at yield σ_y ; (3) extension to failure ϵ_b ; and (4) breaking energy indicated by the area under the curve S_b .

RESULTS AND DISCUSSION

Constrained-Uniaxially Drawn PET

The overall changes in the preorientational behavior of macromolecular chains were evaluated by the measurements of density and birefringence. Figure 2 shows the changes in density with draw ratio (λ). Figure 3 indicates the birefringence of the CU drawn PET corrected by the observed density ($-\Delta n/d$), where two values (parallel and perpendicular to the preextended direction) are compared in order to check the anisotropy. Substantial changes in the molecular packing and orientational behavior occurs at $\lambda > 2.5$. Dumbleton discussed the same phenomenon from the measurement of sonic velocity and described this draw ratio around 2.5, a point at which the orientation of amorphous regions increased to induce crystallization.⁵

Therefore, we expected that such a structural change must be reflected in the tensile properties. In predicting the strain rate dependent responses, two kinds of tensile tests (at extreme deformation speeds, i.e., 1.7×10^{-4} and 13.1 m/s) were performed (Figs. 4-7). From the change in Young's modulus E (Fig. 4), the CU drawn PET shows anisotropy, which becomes prominent at impact speed. The sharp increase at $\lambda > 2.5$ corresponds to a similar increase in birefringence (Fig. 3). The pattern of change in yield strength σ_y (Fig. 5) was almost identical to that of E . The data for breaking strain ϵ_b (Fig. 6) further reveals the anisotropy of

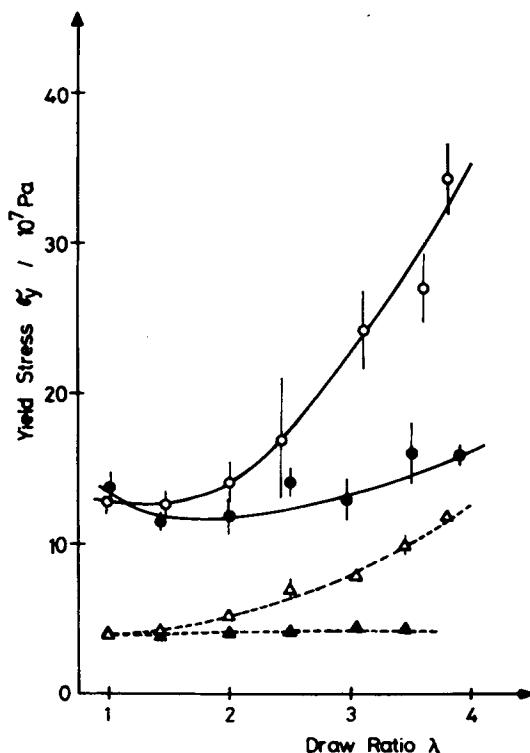


Fig. 5. Dependence of yield strength on draw ratio λ and extension rate $\dot{\epsilon}$ for the constrained-uniaxially drawn PET sheet: (O) (\parallel), (●) (\perp) at $\dot{\epsilon} = 227 \text{ s}^{-1}$; (Δ) (\parallel), (\blacktriangle) (\perp) at $\dot{\epsilon} = 2.9 \times 10^{-3} \text{ s}^{-1}$.

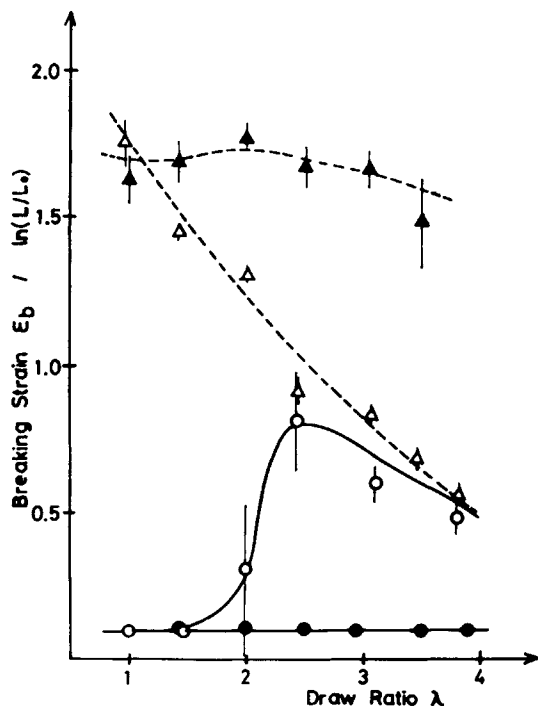


Fig. 6. Dependence of breaking strain on draw ratio λ and extension rate $\dot{\epsilon}$ for the constrained-uniaxially drawn PET sheet: (○) (\parallel), (●) (\perp) at $\dot{\epsilon} = 227 \text{ s}^{-1}$; (Δ) (\parallel), (\blacktriangle) (\perp) at $\dot{\epsilon} = 2.9 \times 10^{-3} \text{ s}^{-1}$.

the sample. At the impact speed, all of the CU drawn PET perpendicular to the preextended direction indicated brittle fracture independent of draw ratios. In the low tensile speed, however, all of the samples deformed uniformly with necking followed by thorough cold drawing. On the other hand, the samples parallel to the preextended direction behaved in a brittle manner at the impact speed up to $\lambda = 1.5$, and began to show ductile deformation at $\lambda > 2$. In the case of the low speed, the sample presented a simple pattern, i.e., ϵ_b decreased in inverse proportion to the preextended quantity. The pattern of the breaking energy S_b changes (Fig. 7) was similar to that of ϵ_b : The breaking energy S_b is roughly equal to the product of σ_y and ϵ_b . While the change in σ_y is a monotonous increase (Fig. 5), the breaking strain ϵ_b varies in a specific way (Fig. 6). Therefore, the product of two (S_b) is dominated mainly by the latter. Thus, the CU drawn PET yielded a considerably different response at various draw ratios, cut-out angles, and tensile speeds.

In the preextended direction the difference of ϵ_b between the low and impact speeds disappeared at $\lambda > 2.5$ (Figs. 6 and 7). There must exist a ductile to brittle transition at $\lambda > 2.5$ in the present range of deformation speeds. To clarify this specific speed region, we examined the strain rate dependent properties of the CU drawn PET parallel to the preextended direction. Figure 8 shows the result of yield stress. The value of σ_y increases approximately semilogarithmically with the tensile speed. The change in Young's modulus was similar to σ_y . On the contrary, the behavior of breaking strain (as well as breaking energy) was not simple and was observed as an abrupt change at a specific tensile speed region

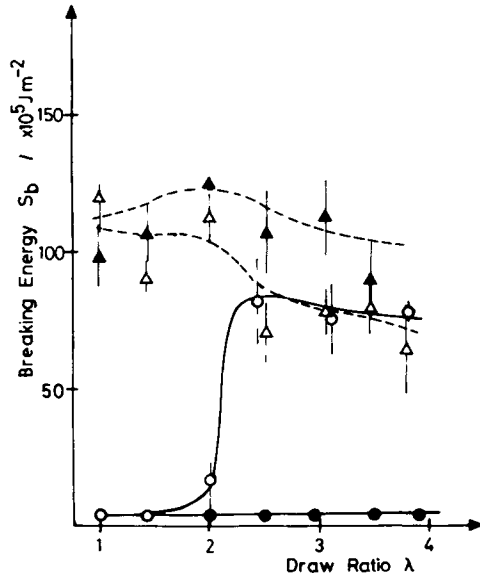


Fig. 7. Dependence of breaking energy on draw ratio and extension rate for the constrained-uniaxially drawn PET sheet: (O) (\parallel), (\bullet) (\perp) at $\dot{\epsilon} = 227 \text{ s}^{-1}$; (Δ) (\parallel), (\blacktriangle) (\perp) at $\dot{\epsilon} = 2.9 \times 10^{-3} \text{ s}^{-1}$.

(Fig. 9). Namely, the undrawn PET showed necking and thorough cold drawing (ductile behavior) until the tensile speed of $1.7 \times 10^{-2} \text{ m/s}$, then the brittle fracture occurred abruptly. This critical deformation speed shifted to a higher speed region (about $2 \times 10^{-2} \text{ m/s}$) in the case of $\lambda = 1.5$, and this tendency was

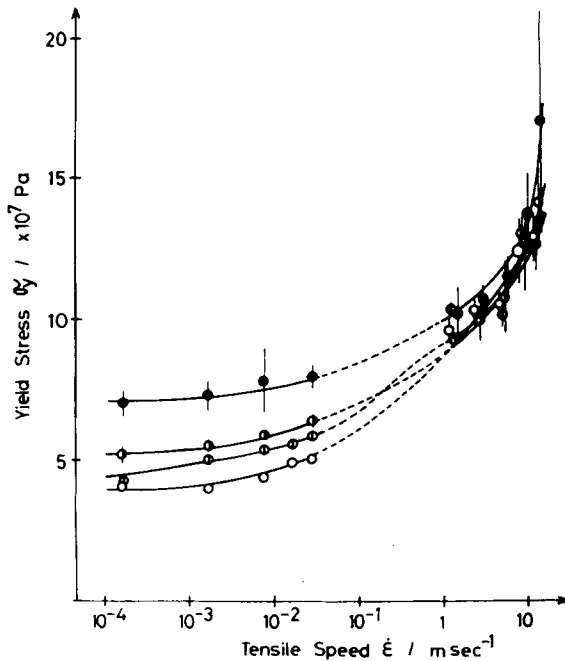


Fig. 8. Strain rate dependencies of yield strength of the constrained-uniaxially drawn PET sheet (\parallel): (O) undrawn; (\odot) $\times 1.5$; (\bullet) $\times 2.0$; (\blacklozenge) $\times 2.5$.

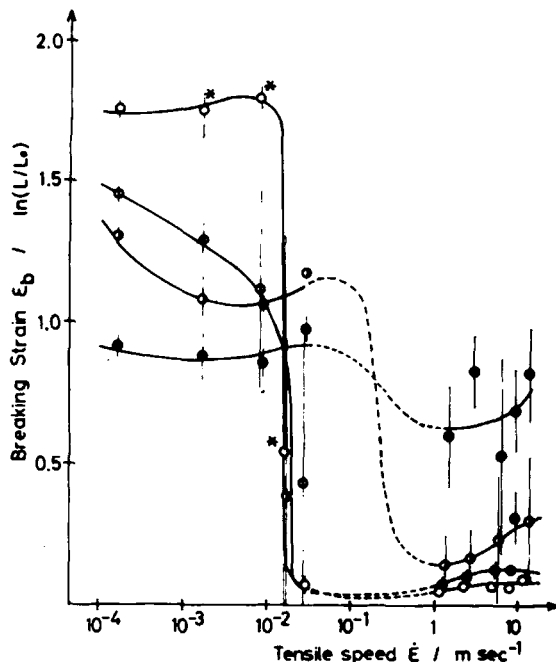


Fig. 9. Strain rate dependencies of breaking strain of the constrained-uniaxially drawn PET sheet (\parallel): (O) undrawn; (\odot) $\times 1.5$; (\bullet) $\times 2.0$; (\bullet) $\times 2.5$.

further promoted for the case $\lambda = 2$. The CU drawn PET at $\lambda = 2.5$ (its birefringence was 2.5×10^{-2}), however, no longer showed any transition, and only ductile behavior was observed. Such a change in tensile behavior illustrated the substantial structural changes at $\lambda > 2.5$.

Next, we observed a specific phenomenon, i.e., serration (self-oscillation of necking), although limited to the undrawn PET sheet. This gave rise to the serrated stress-strain curve, occurring alternately in opaque bands accompanied

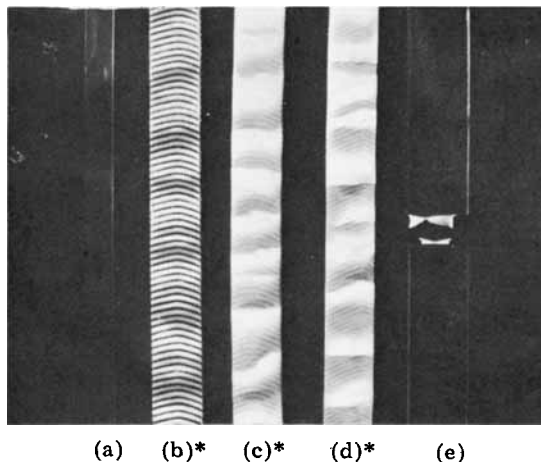


Fig. 10. Photographs of PET during deformation (* serration occurring): (a) $\dot{\epsilon} = 2.9 \times 10^{-3} \text{ s}^{-1}$; (b) $\dot{\epsilon} = 2.9 \times 10^{-2} \text{ s}^{-1}$; (c) $\dot{\epsilon} = 1.4 \times 10^{-1} \text{ s}^{-1}$; (d) $\dot{\epsilon} = 2.9 \times 10^{-1} \text{ s}^{-1}$; (e) $\dot{\epsilon} = 4.8 \times 10^{-1} \text{ s}^{-1}$.

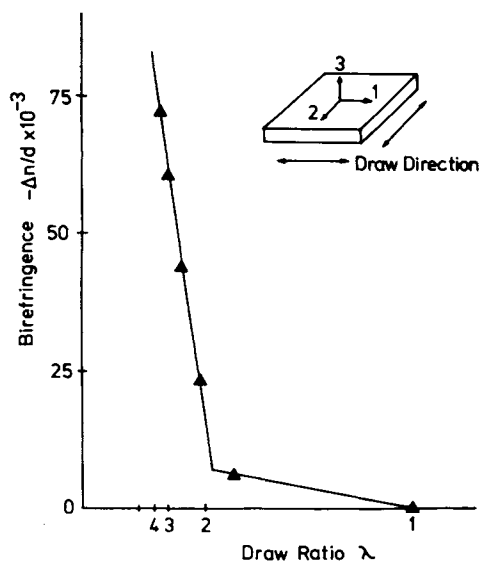


Fig. 11. Change of birefringence [$-\Delta n/d = (n_3 - n_1)/d = (n_3 - n_2)/d$] with drawn ratio for the simultaneous-biaxially drawn PET sheet.

by tremendous voids and transparent bands accompanied by necking and cold drawing at a specific deformation speed (* in Fig. 9). The appearance of the sample varied as a result of the tensile deformation speed: the faster the strain rate, the smaller the fraction of transparent bands (Fig. 10). When the formation

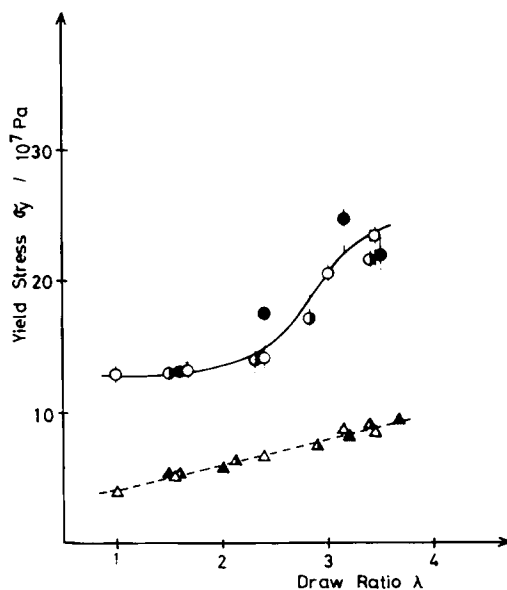


Fig. 12. Dependence of yield strength on draw ratio λ , extension rate $\dot{\epsilon}$, and cut out angle θ for the simultaneous-biaxially drawn PET sheet: (O) $\theta = 0^\circ$; (●) 22.5° ; (●) 45° at $\dot{\epsilon} = 227 \text{ s}^{-1}$; (Δ) $\theta = 0^\circ$; (\blacktriangle) 22.5° ; (\blacktriangle) 45° at $\dot{\epsilon} = 2.9 \times 10^{-3} \text{ s}^{-1}$.

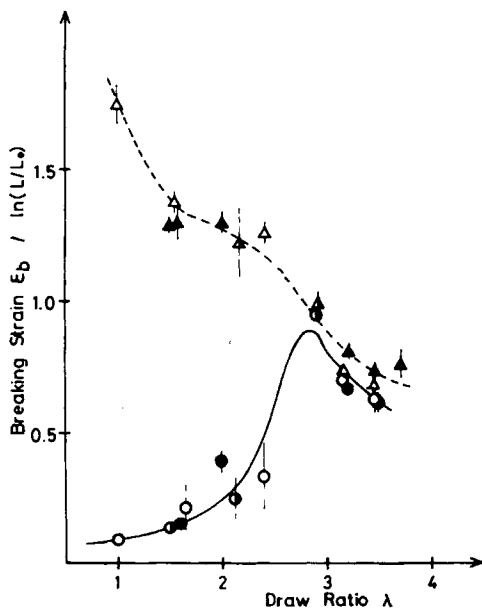


Fig. 13. Dependence of breaking strain on draw ratio λ , extension rate $\dot{\epsilon}$, and cut out angle θ for the simultaneous-biaxially drawn PET sheet: (○) $\theta = 0^\circ$; (◐) 22.5° ; (●) 45° at $\dot{\epsilon} = 227 \text{ s}^{-1}$; (Δ) $\theta = 0^\circ$; (◒) 22.5° ; (▲) 45° at $\dot{\epsilon} = 2.9 \times 10^{-3} \text{ s}^{-1}$.

speed of the opaque bands could no longer follow the strain rate ($1.7 \times 10^{-2} \text{ m/s}$), the sample abruptly underwent brittle fracture. This behavior⁶⁻⁸ has been correlated to a heat transfer problem: The serration is attributed to heat dissipation during necking, corresponding to local temperature jumps and periodic strong variation of elasticity modulus due to poor heat conductivity of the polymer.⁶ A ductile to brittle transition exists as a critical state of the serration. The serration was not observed in the present samples except for the undrawn sheet. Elongation changed the compliance and heat conductivity of the sample and no longer satisfied the strict conditions which induce the serration. However, the ductile to brittle transitions were observed for the drawn sheets with $\lambda = 1.5\text{--}2.5$ (Fig. 9). At present, these transitions represent a critical state of serration and are interpreted by the heat transfer mechanism described above.

Simultaneous-Biaxially Drawn PET

In the previous section, the CU drawn PET exhibits anisotropy and indicates brittle fracture at impact speed regions in the direction perpendicular to the CU drawing direction. These samples, however, formed a structure with strain rate (from low to impact speeds) independent and mechanically superior (tenacious) properties at $\lambda > 2.5$ in the elongation direction. If a sheet were drawn in all directions in order to have the same oriented structure parallel to the CU drawing direction, a mechanically superior sheet could be prepared. This drawing procedure corresponds to the simultaneous-biaxially (SB) drawing. This method was applied to the present undrawn PET sheet. As expected, from the optical

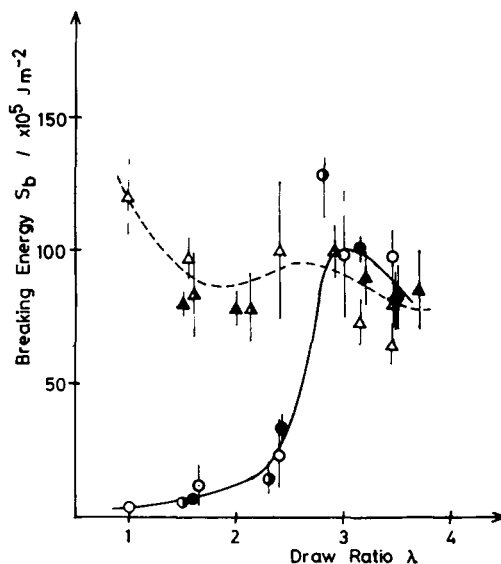


Fig. 14. Dependence of breaking energy on draw ratio λ , extension rate $\dot{\epsilon}$, and cut out angle θ for the simultaneous-biaxially drawn PET sheet: (O) $\theta = 0^\circ$; (●) 22.5° ; (●) 45° at $\dot{\epsilon} = 227 \text{ s}^{-1}$; (Δ) $\theta = 0^\circ$; (\blacktriangle) 22.5° ; (\blacktriangle) 45° at $\dot{\epsilon} = 2.9 \times 10^{-3} \text{ s}^{-1}$.

properties, anisotropy was not observed in the plane of the SB drawing. Figures 2 and 11 show the results of density and birefringence changes due to the SB drawing, respectively. These two figures clearly indicate the common inflection point at $\lambda = 2$. In the tensile testing of the CU drawn samples (Figs. 6 and 7), it was anticipated that the extinction of strain rate dependency will be observed at $\lambda > 2$. The actual experimental results are shown in Figures 12–14 (the tensile speeds were two types, 1.7×10^{-4} and 13.1 m/s). For the SB drawn PET the different tensile behavior due to the cut-out angles ($\theta = 0^\circ$, 22.5° , and 45°) in the sheet plane were not observed. This means the SB drawn sheet is mechanically as well as optically isotropic. Next, it was considered whether the mechanical properties of the SB drawn sheets were inferior to those of the CU drawn sheets. Despite a slight defect in the SB drawing as compared to the CU drawing, the yield strengths of the SB drawn sheet (Fig. 12) were similar in order and tendency of change to those of the CU drawn sheet parallel to the drawing direction (Fig. 5). The changes in breaking strain and energy (Figs. 13 and 14) were analogous to the situation in σ_y described above except that in the case of the SB drawing the strain rate dependency began to disappear at $\lambda >$ about 3 ($-\Delta n/d > 5 \times 10^{-2}$): This value was not in agreement with the corresponding birefringence of the CU drawn sheet at $\lambda = 2.5$ ($-\Delta n/d = 2.5 \times 10^{-2}$). This might be due to the difference in the molecular orientation in the plane of sheet and morphology, but no clear explanation could be offered at the present time. Regarding the PET sheet, the SB drawing at $\lambda > 3$ ($-\Delta n/d > 5 \times 10^{-2}$) can induce a structure with strain rate independent, nonanisotropical, and tenacious properties. The similar situation is presumed for the case of multiaxial drawing, e.g., blow molding. The birefringence value of 5×10^{-2} is a measure of orientation in the biaxial stretch injection blow molding method for plastic bottles made from PET.

CONCLUSION

From the experimental results described above, PET molded products will have excellent mechanical properties if any adequate extrusion or blow molding method accompanying multiaxial orientation with the birefringence $-\Delta n/d > 5 \times 10^{-2}$ is developed.

The authors thank Dr. Mitsui of Teijin Co., Ltd. for the generous supply of amorphous quench-rolled PET sheets.

References

1. M. Yokouchi and Y. Kobayashi, *J. Appl. Polym. Sci.*, **24**, 29 (1979).
2. M. Yokouchi, Y. Hiromoto, and Y. Kobayashi, *J. Appl. Polym. Sci.*, **24**, 1965 (1979).
3. M. Yokouchi, H. Uchiyama, and Y. Kobayashi, *J. Appl. Polym. Sci.*, **25**, 1007 (1980).
4. M. Yokouchi and Y. Kobayashi, *J. Appl. Polym. Sci.*, **26**, 395 (1981).
5. J. H. Dumbleton, *J. Polym. Sci. A-2*, **6**, 795 (1968).
6. G. P. Andrianova, A. S. Kecheqyan, and V. A. Kargin, *J. Polym. Sci. A-2*, **9**, 1919 (1971).
7. V. I. Bekichov, *Vysokomol. Soedin.*, **A16**, 1479 (1974).
8. R. Roseen, *J. Mater. Sci.*, **9**, 929 (1974).

Received January 8, 1981

Accepted June 15, 1981